

Strain-induced g -factor tuning in single InGaAs/GaAs quantum dots

H. M. G. A. Tholen,^{1,*} J. S. Wildmann,² A. Rastelli,² R. Trotta,² C. E. Pryor,³ E. Zallo,^{4,5} O. G. Schmidt,⁴
P. M. Koenraad,¹ and A. Yu. Silov¹

¹*COBRA Research Institute, Department of Applied Physics, Eindhoven University of Technology, P.O. Box 513, NL-5600MB Eindhoven, The Netherlands*

²*Institute of Semiconductor and Solid State Physics, Johannes Kepler University Linz, Altenbergerstraße 69, A-4040 Linz, Austria*

³*Department of Physics and Astronomy and Optical Science and Technology Center, University of Iowa, Iowa City, Iowa 52242, USA*

⁴*Institute for Integrative Nanosciences, IFW Dresden, Helmholtzstraße 20, D-01609 Dresden, Germany*

⁵*Paul-Drude-Institut für Festkörperelektronik, Hausvogteiplatz 5-7, 10117 Berlin, Germany*

(Received 9 May 2016; revised manuscript received 26 September 2016; published 2 December 2016)

The tunability of the exciton g factor in InGaAs quantum dots using compressive biaxial stress applied by piezoelectric actuators is investigated. We find a clear relation between the exciton g factor and the applied stress. A linear decrease of the g factor with compressive biaxial strain is observed consistently in all investigated dots. A connection is established between the response of the exciton g factor to the voltage applied to the piezoelectric actuator and the response of the quantum dot emission energy. We employ a numerical model based on eight-band $\mathbf{k} \cdot \mathbf{p}$ theory to calculate the exciton g factor of a typical dot as a function of strain and a good agreement with our experiments is found. Our calculations reveal that the change in exciton g factor is dominated by the contribution of the valence band and originates from increased heavy hole light hole splitting when applying external stress.

DOI: [10.1103/PhysRevB.94.245301](https://doi.org/10.1103/PhysRevB.94.245301)

Quantum dots (QDs) [1] have often been suggested as fundamental building blocks for future quantum technology, as they can be exploited as sources of single photons or hosts of quantum bits [2]. The single electrons and holes confined to the QDs carry besides a charge also a spin, which can be used to store and process information [3]. Coupling this spin to an externally applied magnetic field leads to an energy difference between the two spin states called the Zeeman splitting. This splitting is generally linear for magnetic fields up to at least 10 T, the highest investigated value in this work. The Zeeman splitting is characterized by the g factor which has a value of 2 for free electrons. However, in a semiconductor crystal the g factor becomes a tensor [4]. The components of this tensor can therefore differ greatly from the free electron g factor of 2. Gaining control over this g tensor is therefore valuable as it implies gaining control of the Zeeman splitting and therewith the spin states.

Moreover, the ability to tune at least one of the components of the g tensor around zero allows for flipping spins [5]. The g tensor depends on the exact electronic structure of the QD and therefore also has a strong dependency on the size and shape of quantum dots [6–8]. This implies that the g tensor in a QD can be manipulated *in situ* by changing its electronic structure, for instance by means of an externally applied electrical or elastic stress field.

Efforts have been made to achieve g -tensor manipulation using external electric fields in InGaAs QDs [9–11]. Here we report the first observation of strain-induced tuning of the g factor of an exciton confined to an InGaAs QD. In our work we apply a magnetic field in the growth direction of the QDs (Faraday geometry), yielding one of the diagonal components of the g tensor, which from now on we will refer to as the (out-of-plane) g factor.

The effects of strain on the electronic structure of semiconductor nanostructures have been extensively studied in the past, both theoretically and experimentally [12–16]. Therefore it is well known that strain profoundly modifies the band structure in a bulk semiconductor material. The main effect is a shift of the band offsets. Furthermore, for nonpurely hydrostatic strain the degeneracy of the valence band is lifted due to a splitting between the heavy hole and light hole bands. In this work we show that the tuning of the exciton g factor can mainly be ascribed to the latter effect.

Several methods to incorporate strain in a QD layer exist, such as by embedding QDs in a bowed airbridge structure [14] or by integrating the QD layer on piezoelectric material [13,17]. The latter method is applied here.

The QDs are grown by solid source molecular beam epitaxy (MBE) [17]. On a GaAs buffer layer we first deposit a 100-nm-thick $\text{Al}_{0.75}\text{Ga}_{0.25}\text{As}$ sacrificial layer, followed by a 150-nm-thick layer of intrinsic GaAs. On top of this, the InGaAs QDs are grown, which are then capped using an indium flush technique [18] to a maximum height of 2.5 nm. The resulting dots have an In concentration of 20%–40%. Finally, the QDs are capped with a 150-nm-thick layer of intrinsic GaAs. By optical lithography and subsequent deposition an etch mask with gold rectangles of size $150 \times 120 \mu\text{m}$ is defined. After etching down to the sacrificial layer the created membranes are released by underetching the AlGaAs layer using HF. Using a flip-chip transfer onto a gold-coated piezoelectric actuator we are able to transfer the membranes to the piezo by gold thermocompression bonding, where the two surfaces are merged by applying simultaneously both force and heat. The used piezoelectric actuator consists of $[\text{Pb}(\text{Mg}_{1/3}\text{Nb}_{2/3})\text{O}_3]_{0.72}\text{-}[\text{PbTiO}_3]_{0.28}$ (PMN-PT).

Using a similar device, Trotta *et al.* [12] were able to vary the in-plane strain ϵ_{\parallel} by as much as $\Delta\epsilon_{\parallel} \sim -0.4\%$, yielding shifts in the QD emission energy of around 15 meV.

A schematic representation of the final sample structure is shown in Fig. 1. The nanomembranes (green) containing

*h.m.g.a.tholen@tue.nl

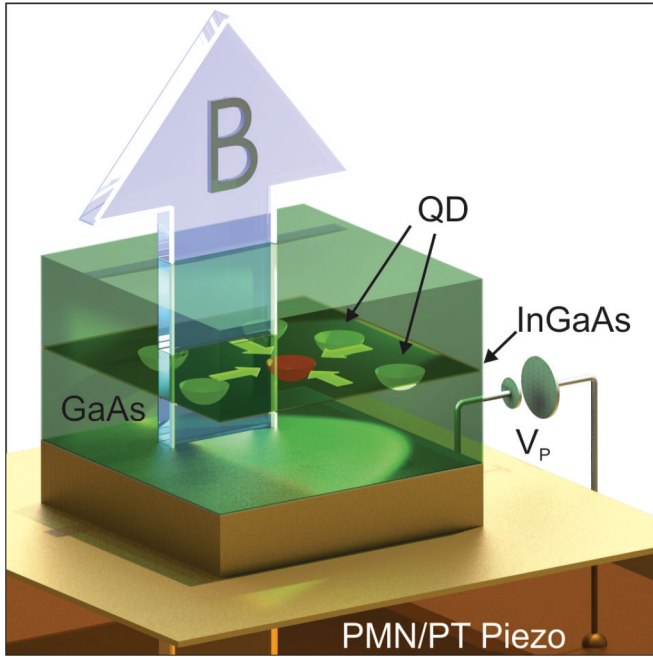


FIG. 1. Schematic layout of the device structure. The InGaAs QDs are embedded in an intrinsic GaAs membrane (green). By means of gold thermocompression bonding this membrane is integrated on top of a piezoelectric actuator, which is used to induce additional biaxial compressive strain (indicated by the green arrows) in the QDs by applying a voltage across the piezo. A magnetic field can be applied in the growth direction of the QDs.

the QDs are bonded onto the piezoelectric actuator, which allows us to induce variable strain by changing the voltage (V_p) between the top and bottom surface of the piezo. Due to the location of the electrodes and the initial poling of the piezo we achieve biaxial compressive strain (ϵ_{\parallel}) by applying a positive voltage to the piezo, indicated by the green arrows. Additional to the strain we are also able to apply a magnetic field (B) parallel to the growth direction of the QDs with a maximal magnitude of 10 T.

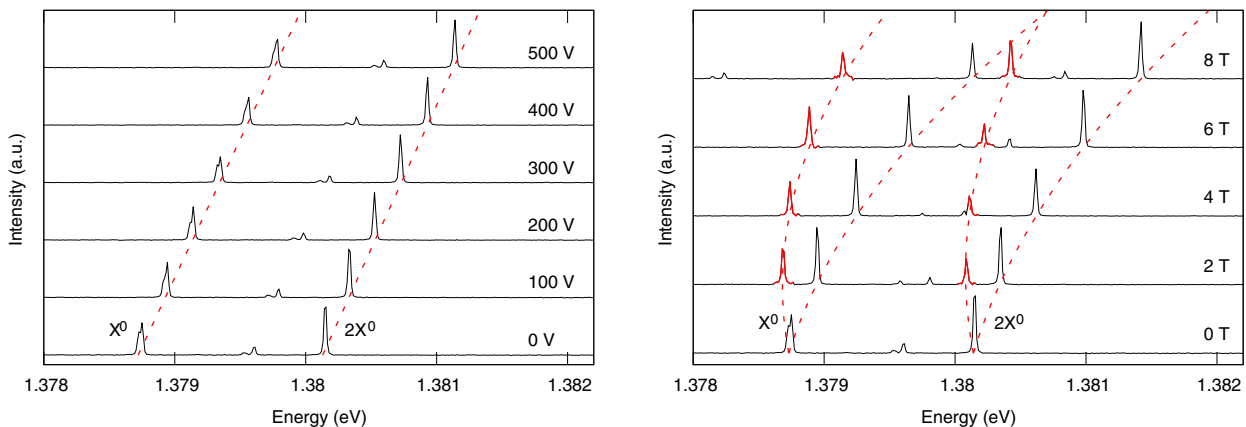


FIG. 2. Left: PL spectra of a single QD as a function of voltage applied to the piezo, where the exciton (X^0) and biexciton ($2X^0$) lines are indicated. A linear regression of the emission energy versus the applied voltage is depicted by the dashed lines. Right: PL spectra of the same QD as a function of magnetic field. The dashed lines indicate the shift and splitting of X^0 and $2X^0$ as a function of magnetic field. Note that the red highlighted peaks have been enhanced five times to increase the visibility.

The use of a diffraction limited confocal microscope, combined with the low QD density in our sample ($\leq 10^6 \text{ cm}^{-2}$), ensures we always illuminate at most one QD. The QDs are excited using a 780 nm laser diode and the photoluminescence (PL) signal originating from the recombined excitons is analyzed using a monochromator with a Si charge-coupled device (CCD). The sample itself is mounted in a low temperature cryostat. The cryostat also contains a liquid helium cooled superconducting magnet, allowing application of magnetic fields up to 10 T along the QDs growth axis.

We will now discuss the influence of strain on the PL signal, which is shown in the left panel of Fig. 2. The X^0 and $2X^0$ peaks were identified by the dependencies of their intensity on the excitation density, which are linear and superlinear, respectively. For this particular dot the $2X^0$ emission is at an higher energy than the X^0 emission, indicating a negative relative biexciton binding energy. For these dots this binding energy can be both positive and negative [12], causing the $2X^0$ emission to be higher in energy than the X^0 emission in some dots and lower in others. Both X^0 and $2X^0$ lines are indicated in Fig. 2 and their energies exhibit a linear shift as a function of applied stress. The relation between the emission energy and the applied voltage can therefore be written as

$$E(V_p) = E_0 + \gamma V_p, \quad (1)$$

where V_p is the voltage applied to the piezoelectric layer and γ is the response of the emission energy to the applied voltage in $\mu\text{eV/V}$. The response of the exciton ($\gamma_{X^0} = 2.07 \pm 0.01 \mu\text{eV/V}$) and the biexciton ($\gamma_{2X^0} = 1.98 \pm 0.01 \mu\text{eV/V}$) are very similar, but not exactly the same. As discussed in detail in Ref. [13], these small differences can be accounted for by the effects of strain on the confinement potential of electron and holes confined in QDs and, as a consequence, on their Coulomb interaction.

In the total range of voltages explored in our experiments (0–500 V), the QD emission lines shift by $\sim 1 \text{ meV}$. Comparing this result with the one achieved by Trotta *et al.* [17] using very similar devices, and neglecting anisotropic stresses, we estimate a change in strain of the order of -0.025% . This is less than the maximum value achieved by Trotta *et al.*, most likely

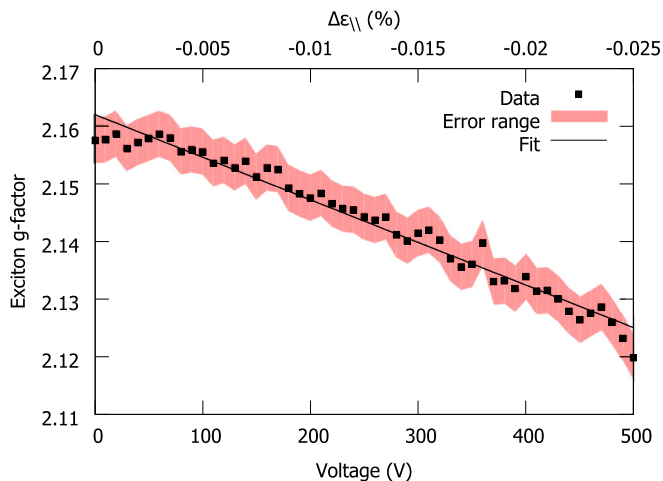


FIG. 3. Exciton g factor of a single QD as a function of applied voltage (e.g., compressive strain), with the linear regression (solid line) and the error range (red area) indicated.

due to the bonding between the piezo and the nanomembranes which can vary from sample to sample. It serves mainly as a guideline to be used for the later calculations.

The right panel in Fig. 2 shows the change of the PL spectrum with magnetic field strength. When exposed to a magnetic field, the emission lines of QDs not only experience a linear Zeeman splitting, but also a quadratic diamagnetic shift. This diamagnetic shift originates from the circulating current that is induced by the magnetic field, creating a magnetic moment, which then couples back to the magnetic field. The quantum dots emission energy E as a function of magnetic field B is therefore given by

$$E(B) = E_0 \pm \frac{1}{2}g_{\text{ex}}\mu_B B + \alpha_d B^2, \quad (2)$$

where E_0 is the energy at zero magnetic field, g_{ex} is the exciton g factor, μ_B is the Bohr magneton, and α_d is the diamagnetic coefficient.

The g factor is determined by fitting Eq. (2) to the data in Fig. 2. As expected this reveals a linear behavior of the Zeeman splitting as a function of magnetic field and for this particular QD the exciton g factor is determined to be 2.158 ± 0.004 . For the other investigated dots, the g factors are of the same order, ranging from 1.4 to 2.4.

The g factor can then be determined as a function of applied stress, which is shown in Fig. 3. This reveals a linear decrease with increasing compressive strain, which is consistent in all investigated dots. The linear dependence reveals that (in the investigated range) we can write the g factor as

$$g_{\text{ex}}(V_p) = g_0 + \chi V_p, \quad (3)$$

where g_0 is the exciton g factor at zero applied voltage and χ is the response of the exciton g factor to the applied voltage.

In order to investigate a possible relation between the response of the g -factor χ and the response of the emission energy γ , Fig. 4 shows χ versus γ for the investigated dots. A relation between the two entities is clearly visible: QDs where the emission energy shows a larger response to strain also have a more responsive g factor.

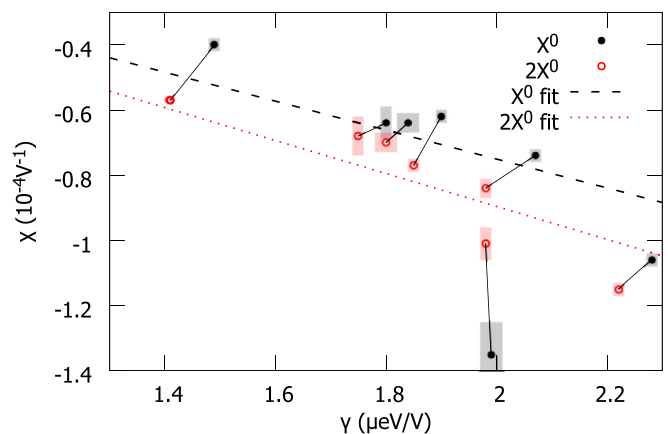


FIG. 4. g -factor response to applied voltage versus the emission energy response for both the exciton and biexciton states of several dots. The dashed lines indicate the respective linear fits. The solid lines pair the excitons and biexcitons originating from the same QD. The shaded areas represent the error ranges.

In general, a dependence exists between the emission energy of a particular QD and its exciton g factor. The ratio between χ/γ , which represents the change in exciton g factor with emission energy, probes the derivative of this dependence at a particular emission energy. Figure 4 thus demonstrates that χ/γ is constant, which implies that the exciton g factor depends linearly on the emission energy. A linear regression reveals a linear dependency of $\chi/\gamma = 0.044 \pm 0.009 \text{ meV}^{-1}$ for the exciton and of $\chi/\gamma = 0.051 \pm 0.006 \text{ meV}^{-1}$ for the biexciton. In Fig. 4 there seems to be a hint of a systematic difference between χ_{X^0} and χ_{2X^0} . When neglecting Coulomb interactions and exchange effects, the biexciton g factor is fully determined by the g factor of the final state, the exciton [19]. In this approximation, the g factors of X^0 and $2X^0$, and their shift with strain, are therefore the same. Taking into account the Coulomb and exchange interactions however, small discrepancies between X^0 and $2X^0$ may be introduced.

In order to better understand our experimental results, we performed numerical calculations for a representative structure, a lens-shaped $\text{In}_{0.4}\text{Ga}_{0.6}\text{As}$ quantum dot with a height of 2.5 nm and a radius of 10 nm, embedded in GaAs. We computed the strain due to lattice mismatch on a cubic grid using continuum elasticity theory. The single-electron energies and wave functions were computed using a real-space eight-band strain-dependent $\mathbf{k} \cdot \mathbf{p}$ model [20,21] on the same cubic grid and using the strain calculated in the first step. With derivatives of the envelope functions replaced by finite differences on the grid, the Hamiltonian becomes a large sparse matrix that was diagonalized using the Lanczos algorithm. Material parameters were taken from Ref. [22] for $T = 0$. Parameters for $\text{In}_{0.4}\text{Ga}_{0.6}\text{As}$ were determined by linear interpolation between InAs and GaAs (Vegard's law), except when Ref. [22] provided bowing parameters (for E_g , Δ , $\gamma_3 - \gamma_2$, E_p , E_v , and a_c). The g factors were determined by computing the Zeeman energy splittings in a uniform magnetic field, coupled to both the Bloch and envelope functions [23,24]. Spurious midgap states [25,26] were eliminated by including an optimized second-nearest-neighbor term [27]. The externally applied strain was included by introducing a

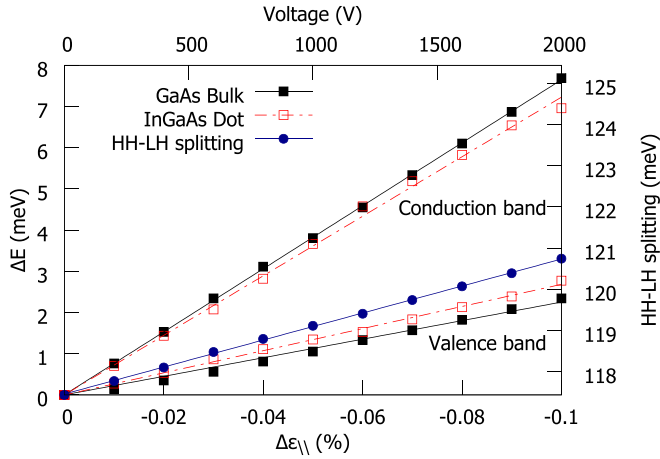


FIG. 5. Change in band-edge energy (calculated values including linear regression) of both the conduction and valence band in the bulk (solid) and the QD (dashed) material as a function of applied strain. It reveals an increase of the band gap in both materials, however larger in the bulk material. The blue line shows the change in the splitting between the heavy hole and light hole bands.

fictitious stressor material at the bottom of the computational grid with a modified lattice constant. The stressor material was given unphysically large elastic constants to ensure that it was not deformed itself by the InGaAs/GaAs quantum dot system. We verified that changing the stressor lattice constant produced the expected biaxial strain in the GaAs immediately above the stressor material. In our calculations the in-plane strain is changed by a maximum value of -0.1% , which is accompanied by an increase of the out-of-plane strain in the opposite direction due to the Poisson effect.

To illustrate the effect of this external strain on the band structure of both the bulk and QD material, Fig. 5 shows the shift of the conduction and valence band edges in both cases. The band edges shift linearly upwards over this range of strain, with the conduction band showing a bigger increase than the valence band, leading to an increase of the band gap energy (~ 5 meV). The band gap of the dot increases less (~ 4 meV). The blue line shows the splitting between the heavy and light hole bands, which increases linearly with strain (~ 3 meV).

These changes in the band structure will lead to a change in the QD's emission energy, which is shown in Fig. 6. By fitting the calculated energies, γ is determined to be $2.37 \pm 0.04 \mu\text{eV}/\text{V}$, agreeing well with the previously found experimental values. The small deviation is most likely due to differences in the exact dot shape, size, and composition and the estimation of the applied strain.

A magnetic field is then applied in the growth (001) direction. It is confirmed that the Zeeman energy is indeed linear in B for magnetic fields up to 10 T. Therefore only one nonzero magnetic field calculation of the electronic states is sufficient. Then using $g_{e,h} = \frac{E_{e,h}^+ - E_{e,h}^-}{\mu_B B}$ the g factor is determined for the electron and hole separately.

We now calculate the hole and electron g factors as a function of strain, which are shown in Fig. 7. From the definition of the g factors in our calculations, the exciton g factor is given by the difference between the two; $g_{\text{ex}} = g_h - g_e$. As the change in hole g factor is about 60 times

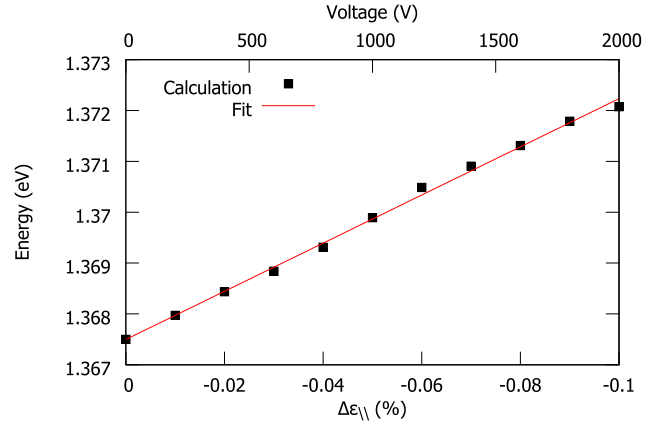


FIG. 6. Calculated energy for the exciton emissions as a function of applied strain. A linear behavior is found as indicated by the solid line, whose slope $\gamma = 2.37 \pm 0.04 \mu\text{eV}/\text{V}$ agrees well with the experiment.

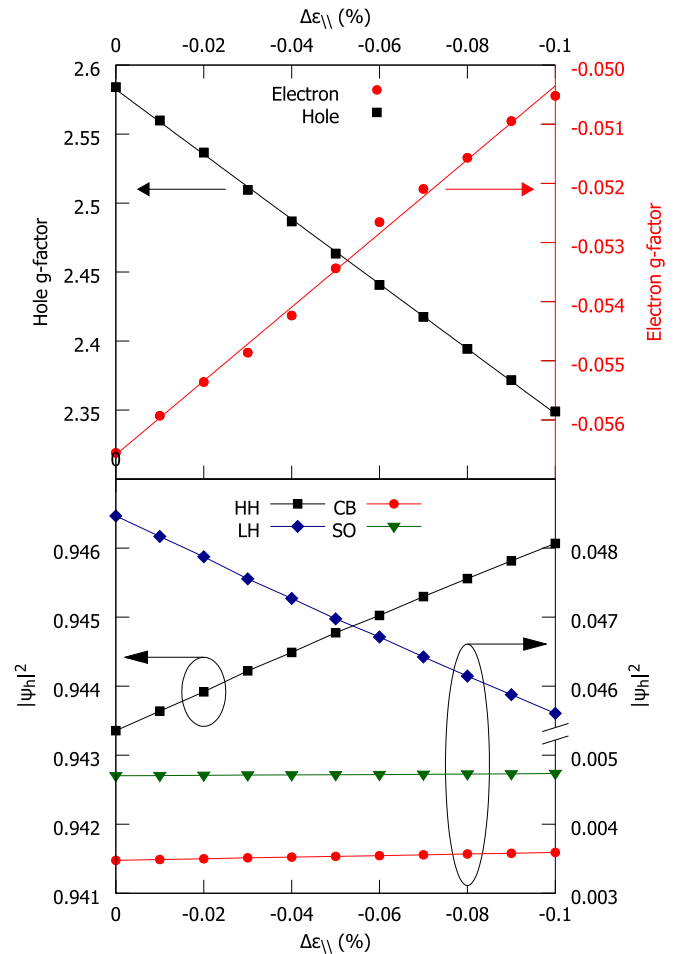


FIG. 7. Top: Calculated hole (open squares) and electron (solid squares) g factor as a function of applied strain. The electron g factor shows a linear increase, however small. The hole g factor has a significantly larger linear strain dependence. The effect agrees with the experiment both qualitatively and quantitatively. Bottom: Composition of the wave function of the hole ground state as a function of the applied strain, revealing that the change in g factor originates from a change in light/heavy hole mixing.

larger than the change in electron g factor we can conclude that the change in exciton g factor is dominated by the valence band contribution. The exciton g factor then shows the same trend as observed in our experiments. From Fig. 7 the value of χ can be determined to be $(-1.21 \pm 0.01)10^{-4} \text{ V}^{-1}$. As both χ and γ depend linearly on the applied strain, the ratio between the two is completely independent of the estimate of strain and therefore allows us to easily compare the outcome of the experiment with the results of the calculations. The ratio between χ and γ is then $0.051 \pm 0.001 \text{ meV}^{-1}$, which is in good agreement with the experimental value we observed.

As the exact value of the g factor is the result of the interplay between the various bands and their mixing into the electron and hole ground states, one must study the wave functions of these states to find the origin of the observed change in the g factor with strain. Here we will analyze only the wave function of the hole ground state, as the strain dependence of the electron g factor barely contributes to the observed change in the exciton g factor. The bottom panel of Fig. 7 shows the contribution of each of the bands (conduction, heavy hole, light hole, and split-off) to the wave function of the hole ground state versus the applied strain. The hole ground state is predominantly of heavy hole character, more than 94%, whereas the light hole band contributes less than 5%. The contribution of the conduction band is small, and more importantly, barely affected by the applied strain. This indicates that the admixture of the conduction band to the valence band states has no significant effect. Instead, a decrease in the contribution of the light hole band to the hole ground state with strain takes place, due to an increased splitting between the light hole and heavy hole states as depicted in Fig. 5. The decrease in the light hole

contribution is compensated by an increase in the heavy hole contribution. We therefore conclude that the change in the g factor originates from a change of light/heavy hole admixture into the hole ground state.

In summary, we have investigated the effect of externally applied strain on the exciton g factor of individual InGaAs QDs. We observed a decrease of the exciton g factor under compressive strain, a trend that was consistent in all investigated dots and reproduced by calculations performed with a numerical model based on strain-dependent eight-band $\mathbf{k} \cdot \mathbf{p}$ theory. The calculation points out that the change in g factor stems from a strain-induced change in the light/heavy hole mixing. The observed changes in the exciton g factor are significant, however relatively small (in the range of several percent). As the strain-induced shift in the emission energy is at least a factor of 15 smaller than what has been reported in literature for similar devices [12,17], we expect that the observed effect can be greatly enhanced. Using novel devices an even larger tuning range will be possible [28–30]. By optimizing the size, shape, and composition of the dots, we can enhance the valence band contribution and improve even further. We therefore anticipate that by engineering QDs exhibiting a small exciton g factor, tuning of this g factor around zero can be achieved and used to gain control over the spin. In a potential application the observed effect could be utilized in combination with external electric fields, to control the spins of the charge carriers using strain while using the electric field to set the charge state of the QD.

This work is part of the Graduate Programme of the Netherlands Organisation for Scientific Research (NWO), Project No. 022.005.011.

-
- [1] P. Michler, *Single Semiconductor Quantum Dots* (Springer, Berlin, 2009), pp. 185–225.
- [2] D. Loss and D. P. DiVincenzo, *Phys. Rev. A* **57**, 120 (1998).
- [3] R. J. Warburton, *Nat. Mater.* **12**, 483 (2013).
- [4] T. P. M. Alegre, F. G. G. Hernández, A. L. C. Pereira, and G. Medeiros-Ribeiro, *Phys. Rev. Lett.* **97**, 236402 (2006).
- [5] J. Pingenot, C. E. Pryor, and M. E. Flatté, *Appl. Phys. Lett.* **92**, 222502 (2008).
- [6] J. van Bree, A. Y. Silov, P. M. Koenraad, M. E. Flatté, and C. E. Pryor, *Phys. Rev. B* **85**, 165323 (2012).
- [7] J. van Bree, A. Y. Silov, P. M. Koenraad, and M. E. Flatté, *Phys. Rev. Lett.* **112**, 187201 (2014).
- [8] J. van Bree, A. Y. Silov, P. M. Koenraad, and M. E. Flatté, *Phys. Rev. B* **90**, 165306 (2014).
- [9] J. H. Prechtel, F. Maier, J. Houel, A. V. Kuhlmann, A. Ludwig, A. D. Wieck, D. Loss, and R. J. Warburton, *Phys. Rev. B* **91**, 165304 (2015).
- [10] F. Klotz, V. Jovanov, J. Kierig, E. C. Clark, D. Rudolph, D. Heiss, M. Bichler, G. Abstreiter, M. S. Brandt, and J. J. Finley, *Appl. Phys. Lett.* **96**, 053113 (2010).
- [11] V. Jovanov, T. Eissfeller, S. Kapfinger, E. C. Clark, F. Klotz, M. Bichler, J. G. Keizer, P. M. Koenraad, G. Abstreiter, and J. J. Finley, *Phys. Rev. B* **83**, 161303 (2011).
- [12] R. Trotta, E. Zallo, E. Magerl, O. G. Schmidt, and A. Rastelli, *Phys. Rev. B* **88**, 155312 (2013).
- [13] F. Ding, R. Singh, J. D. Plumhof, T. Zander, V. Křápek, Y. H. Chen, M. Benyoucef, V. Zwiller, K. Dörr, G. Bester, A. Rastelli, and O. G. Schmidt, *Phys. Rev. Lett.* **104**, 067405 (2010).
- [14] T. Nakaoka, T. Kakitsuka, T. Saito, S. Kako, S. Ishida, M. Nishioka, Y. Yoshikuni, and Y. Arakawa, *J. Appl. Phys.* **94**, 6812 (2003).
- [15] S. Seidl, M. Kroner, A. Hoögele, K. Karrai, R. J. Warburton, A. Badolato, and P. M. Petroff, *Appl. Phys. Lett.* **88**, 203113 (2006).
- [16] E. Zallo, R. Trotta, V. Křápek, Y. H. Huo, P. Atkinson, F. Ding, T. Šikola, A. Rastelli, and O. G. Schmidt, *Phys. Rev. B* **89**, 241303 (2014).
- [17] R. Trotta, P. Atkinson, J. D. Plumhof, E. Zallo, R. O. Rezaev, S. Kumar, S. Baunack, J. R. Schröter, A. Rastelli, and O. G. Schmidt, *Adv. Mater.* **24**, 2668 (2012).
- [18] Z. Wasilewski, S. Fafard, and J. McCaffrey, *J. Cryst. Growth* **201–202**, 1131 (1999).
- [19] A. Kuther, M. Bayer, A. Forchel, A. Gorbunov, V. B. Timofeev, F. Schäfer, and J. P. Reithmaier, *Phys. Rev. B* **58**, R7508 (1998).
- [20] C. Pryor, M.-E. Pistol, and L. Samuelson, *Phys. Rev. B* **56**, 10404 (1997).
- [21] C. Pryor, *Phys. Rev. B* **57**, 7190 (1998).

- [22] I. Vurgaftman, J. R. Meyer, and L. R. Ram-Mohan, *J. Appl. Phys.* **89**, 5815 (2001).
- [23] C. E. Pryor and M. E. Flatté, *Phys. Rev. Lett.* **96**, 026804 (2006).
- [24] A. De and C. E. Pryor, *Phys. Rev. B* **76**, 155321 (2007).
- [25] S. R. White and L. J. Sham, *Phys. Rev. Lett.* **47**, 879 (1981).
- [26] X. Cartoixà, D. Z.-Y. Ting, and T. C. McGill, *J. Appl. Phys.* **93**, 3974 (2003).
- [27] M. Holm, M.-E. Pistol, and C. Pryor, *J. Appl. Phys.* **92**, 932 (2002).
- [28] R. Trotta, J. Martín-Sánchez, I. Daruka, C. Ortix, and A. Rastelli, *Phys. Rev. Lett.* **114**, 150502 (2015).
- [29] R. Trotta, J. Martín-Sánchez, J. S. Wildmann, G. Piredda, M. Reindl, C. Schimpf, E. Zallo, S. Stroj, J. Edlinger, and A. Rastelli, *Nat. Commun.* **7**, 10375 (2016).
- [30] J. Martín-Sánchez, R. Trotta, G. Piredda, C. Schimpf, G. Trevisi, L. Seravalli, P. Frigeri, S. Stroj, T. Lettner, M. Reindl, J. S. Wildmann, J. Edlinger, and A. Rastelli, *Adv. Opt. Mater.* **4**, 682 (2016).